*Invited Paper*

# Development of high power gyrotron and related technologies

Keishi Sakamoto *, Yasuhisa Oda, Ryosuke Ikeda, Takayuki Kobayashi, Ken Kajiwara, Koji Takahashi and Shinichi Moriyama
Japan Atomic Energy Agency, 801-1 Mukoyama, Naka, Ibaraki, Japan 311-0193
* Email: sakamoto.keishi@jaea.go.jp

(Received March 25, 2015)

**Abstract:** The research and development activities of high-power gyrotrons in JAEA for the use in nuclear fusion applications are reported. ITER requires 170 *GHz* 1 *MW* gyrotrons which are currently under development. High order modes of a cylindrical resonator to serve as oscillation mode candidates for 1 *MW*/ 170 *GHz* CW operation are studied. $TE_{31,8}$ mode has shown the best performance operation, e.g., 1 *MW*/ 800 *s*/ 55% and 0.8 *MW*/1 hr/57%. Even higher modes are attempted to increase power. At the present stage, in $TE_{31,11}$ mode, 1.24 *MW*/2*s* and 0.5 *MW*/1000 *s* have been achieved. This 170 *GHz*/$TE_{31,11}$ mode has excellent characteristics for multi-frequency operation. By controlling resonant magnetic field and pitch factor of the electron beam, Gaussian power output was demonstrated at 203 *GHz*, 170 *GHz*, 137 *GHz* and 104 *GHz*. An anode control method was studied as a possible advantage operation scenario. A 5 *kHz* 1 *MW* full-power modulation for the plasma instability suppression was successfully demonstrated at 170 *GHz* by the fast of-off control of the anode voltage. A fast frequency switching of the gyrotron was studied for the power deposition profile control in the tokamak plasma, and the switching between 170 GHz and 167 GHz was proved with 3.5 s using the super-conducting sweeping coil. Furthermore, dual frequency 138 *GHz*/110 *GHz* gyrotron was developed for the application in the EC heating and current drive system of the JT-60SA tokamak. Power outputs of 1 *MW*/100 *s* were demonstrated at both frequencies. High power experiments of the transmission line and launcher were carried out using the gyrotron as a power source.

**Keywords:** High power gyrotron, Multi-frequency, Fast frequency switching, Power modulation

**doi:** 10.11906/TST.001-018.2015.03.01

## 1. Introduction

Gyrotrons are a high-power source of coherent microwaves which use mildly relativistic magnetized electron beams and are based on the cyclotron-resonance maser effect. High-power gyrotrons are used in electron cyclotron heating and current drives (EC H&CD) of the nuclear fusion research in the field of magnetically confined plasma. Their frequencies are in the so-called mm-wave range (28 *GHz*~170 *GHz*), and extensive research and development have been conducted [1-16]. And an even higher frequency >200 *GHz* is proposed in the DEMO reactor [17]. The EC waves are useful not only for H&CD but also for initiating plasmas and active control of MHD instabilities [18-21]. In addition, mm-waves are attractive for fusion reactors, because the mm-waves can be launched into the plasma with high power density through a relatively small hole. Since the gyrotrons can be placed far from the reactor, therefore, maintenance is easy and the system is expected to be highly reliable. The 1 *MW* 170 *GHz* gyrotrons will be used in ITER [22-23]. Their configuration is shown in Fig.1. From the gyrotron building where the twenty-four 1 *MW* gyrotrons are placed, the mm-wave power is transmitted to the plasma by the 24-line evacuated corrugated waveguides. The length of the transmission line is around 150 *m*. The power is injected into the toroidal plasma via two types of the launchers. One is an equatorial port launcher, which has twenty-four mm-wave beam lines and is used for heating and current drive. The other is an upper port launcher, which has eight mm-wave beam lines. ITER has four upper port launchers. Both launchers have steering mirrors to control the power deposition profile in the tokamak plasma. Each transmission line has a waveguide switch for selecting the injection port. The 170 *GHz* gyrotrons require, 1 *MW*, quasi-CW power output having 50% efficiency. Presently, Japan and Russia have demonstrated a gyrotron that satisfies the ITER criteria.

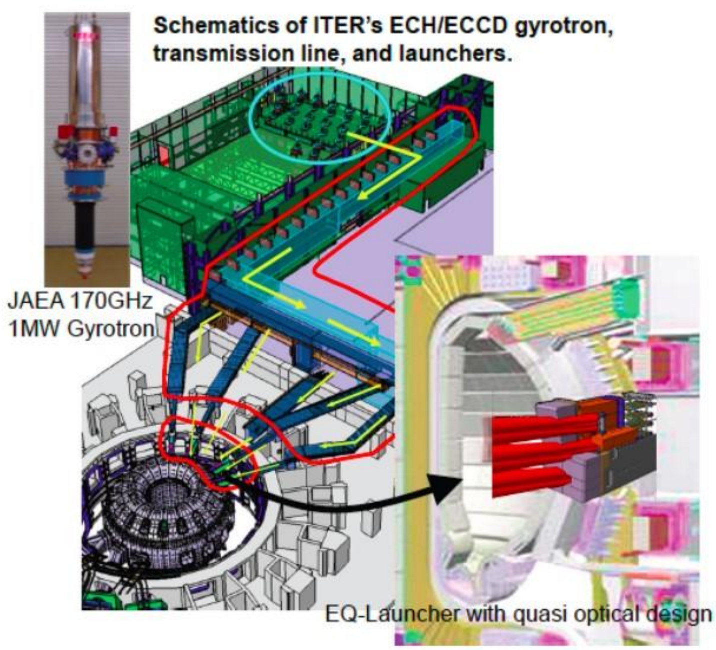


Fig. 1 Schematic view of Electron cyclotron heating and current drive system of ITER with 170 *GHz* 1 *MW* gyrotron. A height and weight of the gyrotron is ~3 *m* and 800 *kg*, respectively.

Modern high-power gyrotrons consist of an electron gun (magnetron injection gun: MIG), beam tunnel, cavity (resonator), built-in mode converter, diamond window for power output and a collector, and are inserted in a solenoid super-conducting magnet (SCM). The electron gun emits an annular electron beam of 60 *keV*~90 *keV*. Each electron has a gyro-motion at the cavity with a pitch factor of about 1.0~1.4. By adjusting the resonance magnetic field and the beam position in the cavity, the oscillation of the objective mode is obtained. The power conversion efficiency from the electron beam to the microwave is 30~40%. A part of the residual power of the electron beam after the cavity interaction is recovered using a retarding potential between the cavity and the collector (depressed collector configuration).

In JAEA, the first 170 *GHz* gyrotron aiming for 1 *MW* power output was fabricated in 1995. The oscillation mode was $TE_{31,8}$ mode, and 1 *MW* (1 *ms*) oscillation was demonstrated in 1996. A diamond window was first installed in 1998. Pulse duration and output power increased by improving the MIG, beam tunnel, the quasi-mode converter, stray radiation treatment, and a 1 *MW*, >50%, quasi-CW operation was demonstrated in 2006. After demonstrating the ITER-relevant 1 *MW* 170 *GHz* gyrotron, higher power gyrotrons, multi-frequency gyrotrons and advanced operation technologies continued to be developed.

The 110 *GHz* gyrotron were used in the EC system of the JT-60U tokamak in 1999, and currently dual frequency gyrotrons for the JT-60SA tokamak are being developed.

EC technology such as high-power mm-wave transmission components [24-29] and power supplies for advanced gyrotron operation are also being developed in parallel.

In this paper, development activities of advanced high-power gyrotrons are described. Sections 2 and 3 describe the design of the 1 *MW* 170 *GHz* gyrotrons as well as the multi-frequency gyrotrons. The result of full-power modulation using an anode switch is shown in section 4. Section 5 introduces the activities for applying the electron cyclotron heating and current-drive to the ITER, while section 6 summarizes the paper.

## 2. High-power 1 *MW* 170 *GHz* gyrotrons

R&D of the 1 *MW* 170 *GHz* gyrotrons started with the $TE_{31,8}$ oscillation mode in a cylindrical open cavity. This mode was selected as the minimum mode number to generate 1 *MW* CW oscillation at 170 *GHz*, i.e., the heat load on the inner surface of the cavity is suppressed to the level of ~20 $MW/m^2$. After ITER-relevant parameters were demonstrated [11], the oscillation mode number was increased to relax the Ohmic heat load on the inner wall of the cavity. The tested modes were $TE_{31,9}$, $TE_{31,11}$ and $TE_{31,12}$. As the frequency (f=170 *GHz*) and the m-number of the $TE_{m,n}$ mode are the same (m=31), the beam position $r_b$ ($=r_{cav}\chi_{m-1,1}/\chi_{m-1,n} \sim c\chi_{m-1,1}/(2\pi f)$) in the cavity is the same, and the beam trajectory is the same among these modes. Therefore, components having identical designs such as the MIG, beam tunnel, collector, and 7 *T* solenoid coil are available with the exception of the cavity and the mode converter/mirrors. Here, $r_{cav}$ :a cavity radius, $\chi_{m,n}$ : n-th root of m-th Bessel function $dJ_m(x)/dx=0$, f: frequency, c: light velocity.

**2-1 Gyrotron setup and quasi- CW highly efficient oscillation**

A picture of a 170 *GHz* gyrotron is shown in Fig.1 and is approximately ~3 *m* in height and weights ~800 *kg* including the X-ray shield around the collector. A schematic view is shown in Fig.2. The gyrotron is inserted in the SCM that has a room temperature bore of 240 *mm*. The hollow electron beam is generated by a triode type MIG and the diameter of the emission belt is 93 *mm*. The electron beam is transported for 400 *mm* downstream to the cavity. The cavity radius is 17.9 *mm* to excite the $TE_{31,8}$ mode and the beam radius is 9.13 *mm*.

Tab. 1 Mode content at the output of the in-waveguide mode converter

| Mode | Contents(%) |
|---|---|
| TE24,10 | 2.2 |
| TE25,10 | 3.7 |
| TE26,10 | 4.4 |
| TE27,10 | 2.2 |
| TE26,9 | 1.2 |
| TE27,9 | 6.7 |
| TE28,9 | 10.1 |
| TE29,9 | 13.5 |
| TE30,9 | 5.2 |
| TE31,9 | 1.7 |
| TE29,8 | 2.7 |
| TE30,8 | 6.4 |
| TE31,8 | 12 |
| TE32,8 | 10.2 |
| TE33,8 | 2.8 |
| TE33,7 | 3.3 |
| TE34,7 | 3.6 |
| TE35,7 | 2.4 |

The $TE_{31,8}$ mode is converted to a single peaked power profile using the in-waveguide converter (radiator), and formed to a Gaussian-like parallel beam by the parabolic mirror, and transmitted to the window using three mirrors as shown in the figure. The power is outputted through a diamond window. A thickness is 1.853 *mm*. The inner surface of the in-waveguide converter has dimple shape (see Fig.2) to convert the original oscillation mode to the many modes combination to form a single peaked power profile. The mode contents are shown in Table 1. Approximately 18 modes are generated from the single $TE_{31,8}$ mode, and the final content of $TE_{31,8}$ mode is only 12 % at the output. A $Si_3N_4$ cylinder is installed as a DC insulator between the body and the collector to apply the bias voltage for the depressed collector. Here, the collector is grounded and a high positive voltage 25~30 *kV* is applied to the body section. The body is covered with the insulator (blue part of the gyrotron seen in Fig.1).

The triode MIG has an advantage that the beam voltage and the pitch factor of the electron beam can be controlled independently, therefore, which enables an active control of the beam parameters during the oscillation to access to the operation point of the maximum efficiency easily. The output power couples with the 63.5 *mm* diameter waveguide of via mirrors in the MOU, where 94.5% of the output power was transmitted to a dummy load. Here a power loss in the MOU was ~4.5%.

This gyrotron was the first to provide 1 *MW* quasi-CW operation. High efficiency oscillation was achieved in the so-called hard excitation region using the active control of the operation parameters (the resonance frequency at the cavity and the electron beam pitch factor), e.g., 55% at 1 *MW*, 57% at 0.8 *MW* (1 hour operation) and 60% at 0.6 *MW*. In the quasi-CW operation, the vacuum pressure in the tube reached to a stable value [11].

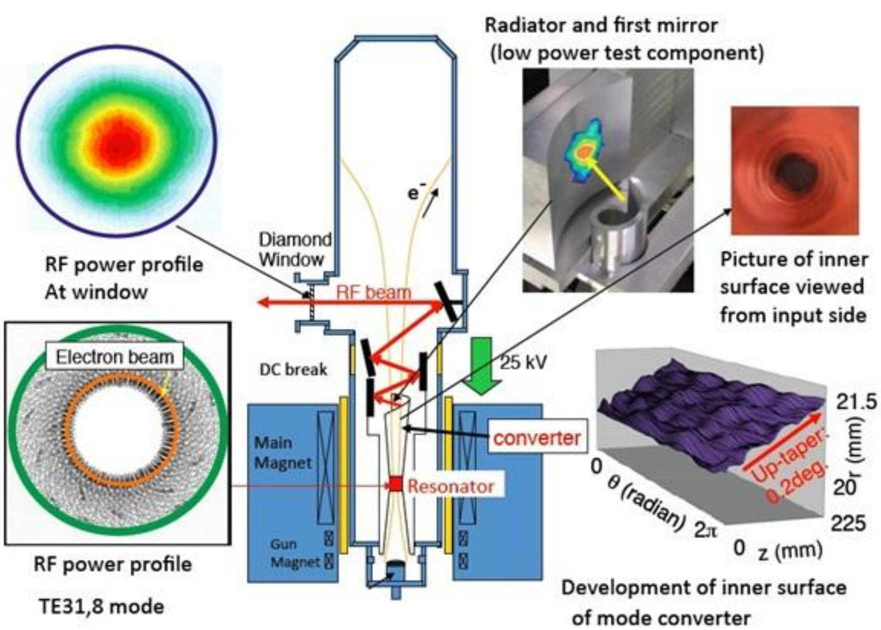


Fig. 2 Schematic view of the gyrotron and inner RF components and RF profiles in the cavity (TE31,8 mode) and at the window

In actual operation, repetitive operation is unavoidable. The EC system was tested for reliability by highly repetitive operation of the 170 *GHz* gyrotron. An 800 *kW*/ 600 *s* pulse was repeated at an interval of 20~30 *min* at the 52-57% electrical efficiency, which is expected operation interval of ITER. The beam voltage $V_{beam}$ and beam current $I_{beam}$ were ~67 *kV* and ~34 *A*, respectively, and the depressed collector voltage $V_{dep}$ was ~24 *kV*. Seventy-two shots of the 88 trial shots had successful 600 *s* oscillation without being terminated intermediately. The 16 unsuccessful shots were interrupted for reasons such as a light emission in the tube, an abrupt beam current increase, or a mode transition to an adjacent mode [13]. To further increase the system operation ratio, a rapid recovery scenario method should be realized without a sequence stop. A pitch factor control and/or beam current control using an anode voltage control will be a powerful tool for this purpose. Developing an operation rapid recovery scenario is a major theme for a long pulse gyrotron systems.

This gyrotron has been functioning since 2006 and has recorded an output energy of >250 *GJ* and its achievements compared too other gyrotrons are summarized in Table 2 with other gyrotrons.

**2-2 Power modulation using anode voltage switching of the triode gun**

A 5 *kHz* full power modulation experiment was performed on a 170 *GHz* gyrotron. The gyrotron beam current depends on the voltage between the anode and cathode $V_{ak}$ of the triode MIG as shown in Fig.3(a), i.e., the beam current $I_b$ shows a nominal value when the switch is open, and $I_b$=0 when closed. Using the beam current switching, 5 *kHz* power modulation was tried. The configuration of the system is shown in Fig.3(b). This method has following advantages. As the beam current is zero at no oscillation phase, collector heat load could be suppressed to half, X-ray decreases, and the total averaged efficiency increases. As the averaged heat deposition to the cavity is also half, the power can be increased compared to the CW operation.

Tab. 2 Status of 170 *GHz* gyrotron performances in JAEA

| Mode (Power limit) | Power | Pulse | Efficiency | |
|---|---|---|---|---|
| TE31,8 (1.0 *MW*) | 1 *MW* | >800 *s* | 55% | |
| | 0.8 *MW* | 3600 *s* | 57% | |
| | 0.6 *MW* | 300 *s* | 60% | |
| TE31,9 (1.2 *MW*) | 1 *MW* | 1 *ms* | 32% | w/o CPD |
| | 0.6 *MW* | 10 *s* | 51% | |
| TE31,11 (1.6 *MW*) | 1.24 *MW* | 2 *s* | 45% | |
| | 1 *MW* | 200 *s* | 46% | |
| | 0.6 *MW* | 1000 *s* | 47% | |
| | 0.6 *MW* | 2 *s* | 50% | |
| TE31,12 (1.8 *MW*) | 1.56 *MW* | 1 *ms* | 27% | w/o CPD |
| | 1.03 *MW* | 2 *s* | 40% | |
| | 0.55 *MW* | 200 *s* | 42% | |
| | 0.94 *MW* | 50 *s* | - | At NFRI [30] |

(w/o CPD: operation without depressed collector)

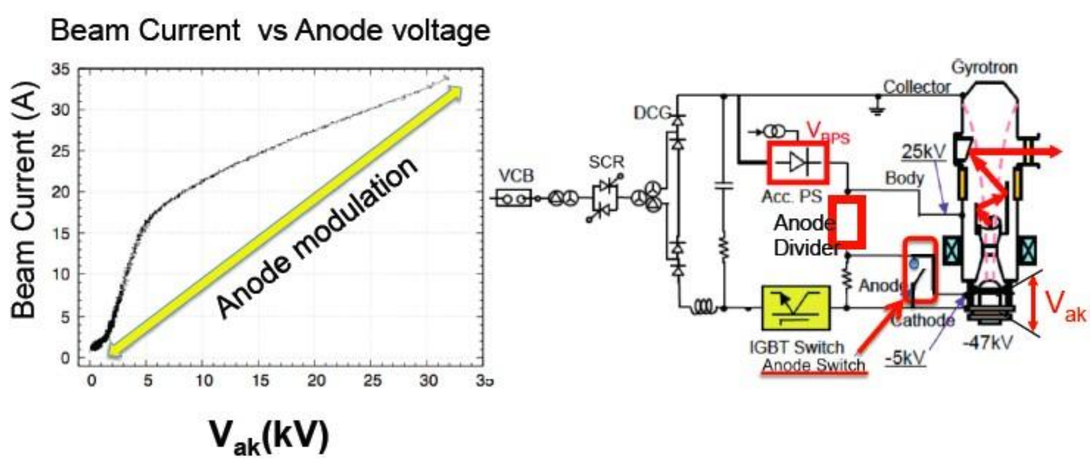


(a) (b)

Fig. 3 (a) Dependence of the beam current on the voltage between the anode and cathode of the triode MIG. (b) Configuration of the power supply system with the fast switch between anode and cathode

In the experiment, the 5 *kHz*/60 *s* operation was demonstrated successfully [16]. The maximum power achieved was 1.16 *MW* having an electrical efficiency of 48%.

At the start-up phase of each pulse, if the anode voltage or current ramp-up time is slow, it will cause a longer duration time of the lower mode (lower frequency). This is not preferable both for the application and for the collector heat load since high-power electron beam deposition occurs. To make the anode voltage rise faster, another fast switch was inserted between the anode voltage divider and the anode (double anode switch) as shown in Fig.4. This cut the stray capacity of the anode feeding circuit, and as a result, unwanted charge/discharge was avoided. Fast start-up of the anode voltage was successful and unwanted mode generation was minimized.

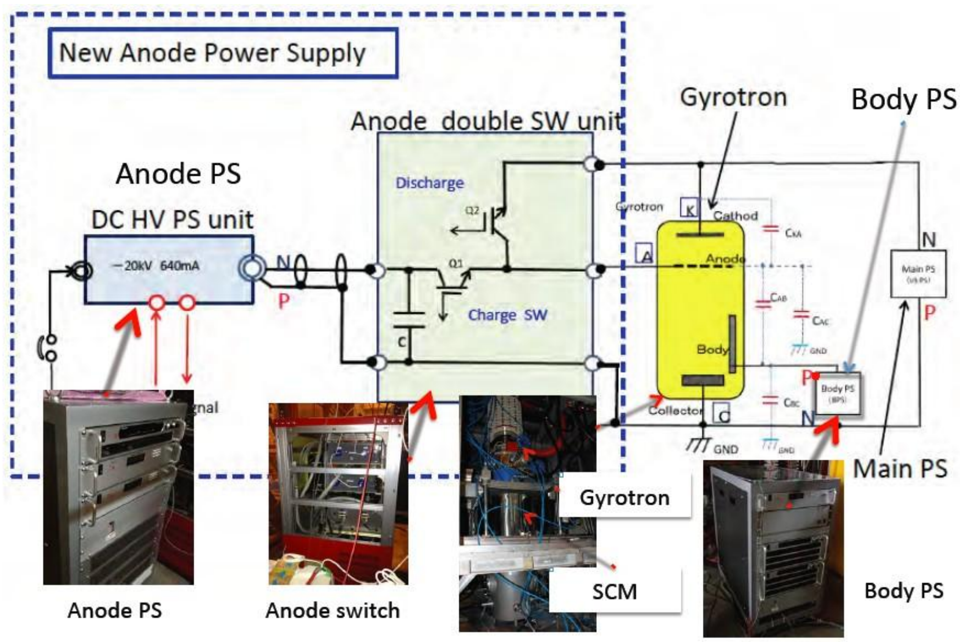


Fig. 4 Configuration of the power supply with dual anode switch for 5 kHz CW power modulation.

## 3. Multi-frequency gyrotron having triode magnetron gun

### 3-1 170 *GHz* $TE_{31,11}$ mode gyrotron and its multi-frequency operation

A170 *GHz* $TE_{31,11}$ mode gyrotron was fabricated for application in ITER. Fig.5 is a picture of the gyrotron with the SCM and MOU (matching optics unit) and oil tank for high voltage DC power feeding to the cathode, anode and body terminals.

Many components of the $TE_{31,11}$ mode gyrotron such as the MIG, beam tunnel, the collector, the output window (diamond disk), and the insulator for the depressed collector have the same design as the $TE_{31,8}$ mode gyrotron. The cavity radius is 20.87 *mm*. The peak heat load of the cavity is low compared to the $TE_{31,8}$ mode, so the 1.6 *MW* will be possible for the cavity. The in-waveguide mode converter design is optimized for $TE_{31,11}$/170 *GHz*. Since the bounce angle of the $TE_{37,13}$/203 *GHz*, $TE_{25,9}$/137 *GHz* and $TE_{19,7}$/104 *GHz* are the same as the $TE_{31,11}$/170 *GHz*, the mode converter acts similarly for these modes. That is to say, the Gaussian-like beam is formed at the window. These frequencies match the penetration condition of the diamond window of 1.853 *mm* (=n*$\lambda_g$/2, $\lambda_g$ : wavelength in the material, n: integer). Furthermore, the electron beam position and the pitch factor in the cavity can be optimized to excite the target mode by selecting the optimum parameters of the MIG field $B_{MIG}$ and the anode voltage of the triode MIG, therefore, the ideal multi-frequency gyrotron will be realized. In Table 3, azimuthal bounce angle $\theta_w$, diamond transparent frequency at 1.853 *mm* in thickness and typical design operation parameters: beam position $r_b$, cavity field $B_c$., $B_{MIG}$, $V_{ak}$, pitch factor, are summarized for operation modes and frequencies. On the 170 *GHz* experiment, 1.24 *MW*/2 *s*, 0.6 *MW*/2 *s*/50%, and 0.6 *MW*/1000 *s*/47%, etc. were obtained. By optimizing the cavity field $B_c$, $B_{MIG}$ and the anode voltage, the 1 *MW* outputs with Gaussian-like RF beams were obtained both at 137 *GHz* and 104 *GHz*. In addition, recently, the Gaussian output of 203 *GHz* was also demonstrated at center of the window as designed.

Fig. 5 Picture of ITER relevant gyrotron, SCM matching optics unit, oil tank.

### 3-2 Dual frequency gyrotron for EC H&CD system of JT-60SA

The JT-60SA, an international project between Japan and EU, is currently under construction. Conceptual picture is shown in Fig.6(a). The toroidal magnetic coils are super conducting magnets. The major radius of the torus is ~3 *m*. And the pulse duration is 100 *s*. The EC H&CD system is expected to be a local electron cyclotron heating system. Power injection of 7 *MW* is expected with nine 1 *MW* gyrotrons. The frequencies will be determined from the requirements of the JT-60SA experiment. In Fig.6(b), the cross sectional view of the JT-60SA vacuum vessel and toroidal plasma is shown along with the position of second harmonic electron cyclotron resonance frequencies. Here, the toroidal magnetic field at the plasma center is $B_t$~2.25 *T*. To perform both the center and edge heating experiments, a dual-frequency gyrotron operating at 110 *GHz*/ 138 *GHz* is expected. The oscillation modes are $TE_{22,8}$ for 110 *GHz*, and $TE_{27,10}$ for 137.5 *GHz* [31].

Tab. 3 Operation modes for multi-frequency oscillation and these frequencies, azimuthal bounce angle $\theta_w$, diamond transparent frequency at 1.853 *mm* in thickness and typical design operation parameters beam position $r_b$, cavity field $B_c$., $B_{MIG}$, $V_{ak}$, pitch factor at the beam voltage of 72 *kV*

| Mode: TE(m,n) | Oscillation frequency | $_w$(deg ) | Transparent frequency | $r_b$(mm) | $B_c$(T) | $B_{MIG}$(T) | $V_{ak}$(kV) | Pitch factor |
|---|---|---|---|---|---|---|---|---|
| (37,13) | 203 *GHz* | 65.3665 | 204 *GHz* | 9.1 | 7.93 | 0.31 | 49 | 1.35 |
| (31,11) | 170 *GHz* | 65.3492 | 170 *GHz* | 9.13 | 6.64 | 0.28 | 42 | 1.35 |
| (25,9) | 137 *GHz* | 65.3235 | 136 *GHz* | 9.19 | 5.35 | 0.21 | 36 | 1.35 |
| (19,7) | 104 *GHz* | 65.3003 | 102 *GHz* | 9.25 | 4.06 | 0.172 | 28 | 1.32 |

The cavity radius is 22.8 *mm*. A thickness of the diamond window is 2.29 *mm*. The basic configuration and the outer size are the same as the 170 GHz gyrotrons. Stable 100 s operation was obtained, which satisfies the final objective of the JT-60SA requirements. Because of the restrictions of the power supply (minimum voltage of the man power supply is ~62 *kV*), the total efficiency is limited below 50%, however, the oscillation efficiencies are 34% and 32% for 110 *GHz* and 138 *GHz*, respectively. In Fig.7, there is a conceptual view of the EC system on JT-60SA.

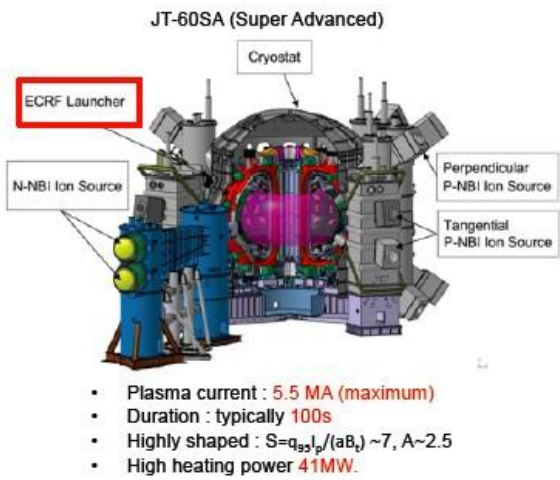


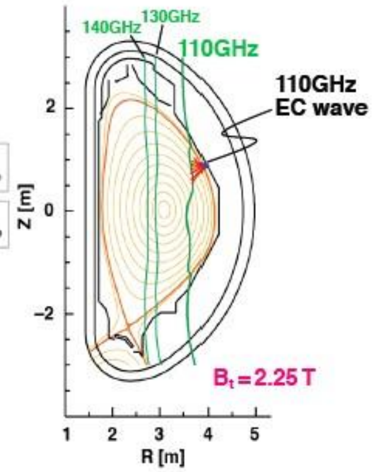


(a) (b)

Fig. 6(a) Conceputual picture of JT-SA tokamak. (b) Cross sectional view of the tokamak and the position of the electron cyclotron resonances for 110 *GHz*, 130 *GHz*, and 140 *GHz*

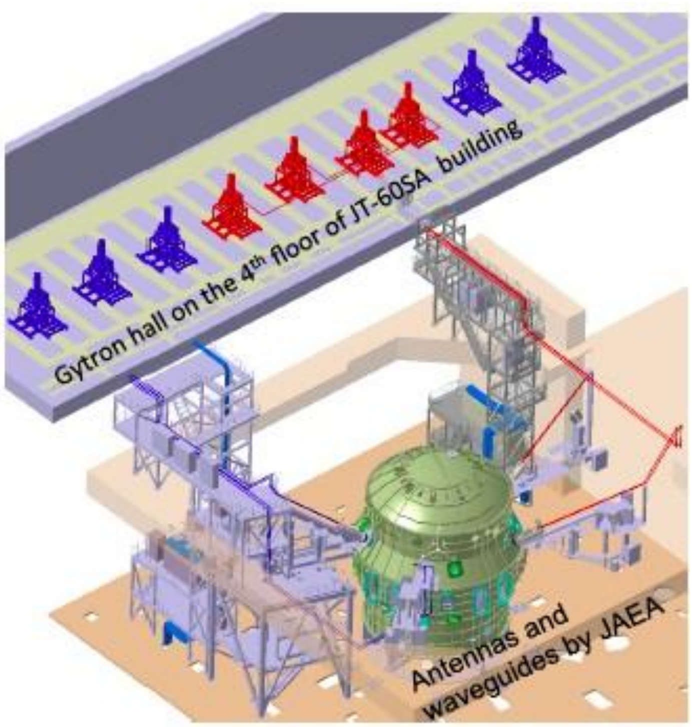


Fig. 7 Conceptual drawing of the gyrotron array in the Gyrotron hall and the JT-60SA hall.

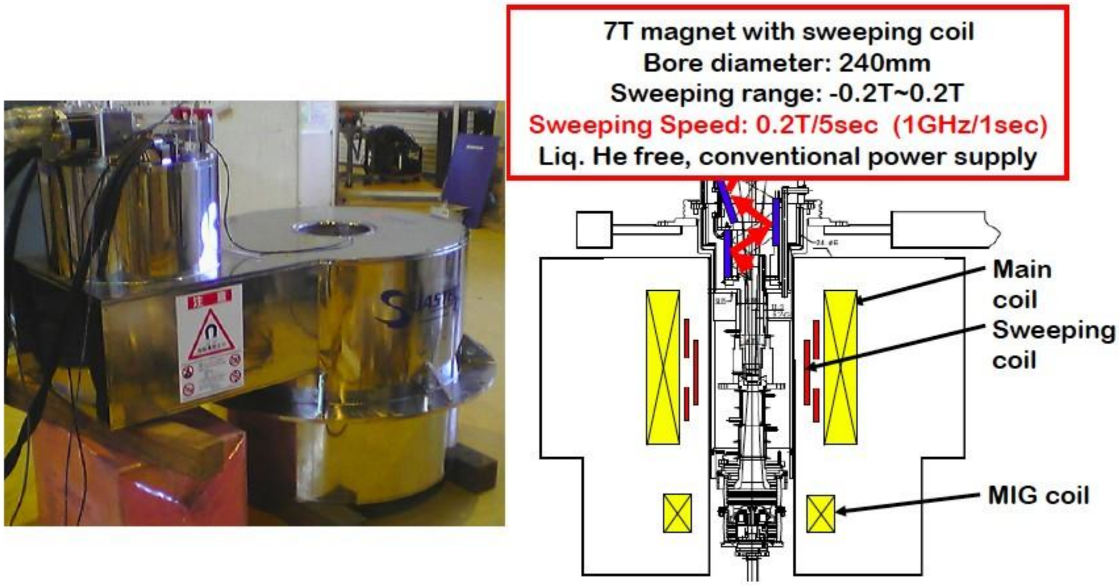


(a) (b)

Fig. 8 (a) Picture of Liquid-He free 7 *T* super conducting magnet (SCM). (b) Cross sectional view of the 7 *T* SCM. The sweeping coil is made of $Sn_3Nb$, and others are NbTi.

### 3-3 Fast step tunable operation with superconducting auxiliary coil

The role of the EC H&CD is the power deposition profile control in the tokamak plasma. For this purpose, the mirror angle steering is commonly adopted as shown in section.5. Alternative method is a fast frequency switching of the gyrotron. Fast control of the gyrotron frequency is firstly demonstrated in KIT by changing the $B_c$ using the inner sweeping solenoid coil [32]. In JAEA, the SC sweeping coil of SCM is employed [33], therefore, the frequency control system in CW operation is available. The magnet consists of three sets of coils; NbTi main coil, NbTi gun coil and $Nb_3Sn$ sweeping coil. Fig.8 shows the SCM and its inner coil configuration. The sweeping speed is 0.2 *T*/5 *sec* using a commercial power supply, which corresponds to ~1 *GHz*/s. The room temperature bore diameter is 240 *mm*. First experiment was conducted using the $TE_{31,8}$ gyrotron. In Fig.9, a time trace of the frequency control experiment is shown. Here, $V_b$ is fixed at 71.0 *kV*, and $I_b$=27.4 *A*. The frequency shifted between 170 *GHz* and 167 *GHz* at 3.5 *s*. The oscillation modes were $TE_{31,8}$ and $TE_{30,8}$, respectively. The power and the efficiency without the depressed collector are 615 *kW* (32 %) and 538 *kW* (27%), respectively. This makes it a prospect to be used in the power deposition control system that aims for plasma stabilization of magnetically confined plasma. Because the magnetic filed strength decreases towards the major radius direction in the case of tokamaks, the power deposition point can be controlled by controlling frequencies. Consequently, a very simple power injection system will be available without a complex rotational mirror in the mm-wave launcher. For reference, the power deposition point moves roughly ~10 *cm* by 3 GHz frequency shift in the plasma for the ITER class tokamak.

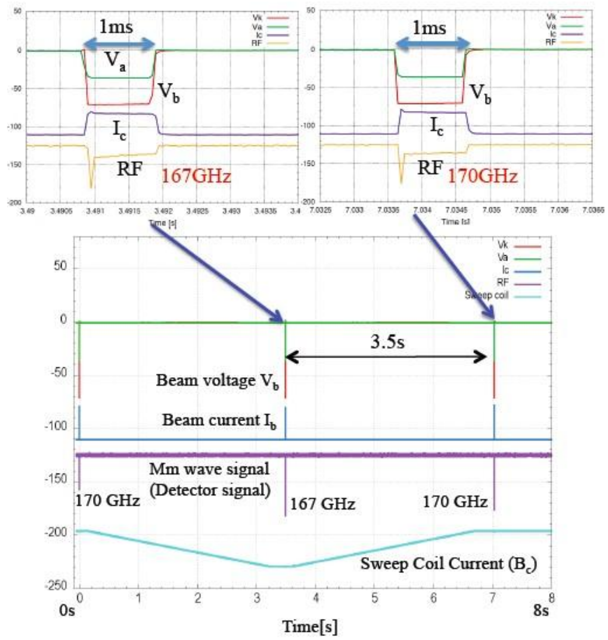


Fig. 9 Time traces of beam voltage $V_b$, beam current $I_c$, *mm*-wave signal detected by diode and sweeping coil current which corresponds to the change of the cavity field. At the bottom of the sweeping current, the $TE_{30,8}$ mode (166.8 *GHz*) was excited. Pulse duration of the pulses is 1 ms as indicated in upper figures.

## 4. Transmission and launching system

### 4-1 Transmission experiment [34, 35]

The output power from the gyrotron can be utilized as a high power source for the R&D of the transmission line and the launcher. Fig.10 shows transmission line composed of the evacuated waveguide (63.5 *mm* in diameter) with 6 miter bends and one waveguide switch, polarizer, directional coupler, evacuation system, in which a simulation of the ITER system is available. The output power from the gyrotron couples with the waveguide via MOU. As the power profile of multi-frequency gyrotron is located in the center of the window, good coupling is expected for multi frequencies. As an example, coupling of the millimeter-wave output of the multi-frequency gyrotron with the transmission line was tried. Here, the tested frequencies are 170 *GHz* and 137 *GHz*. Using two RF beam reflecting mirrors in a matching optics unit (MOU), which are designed to transform the beam profile of the gyrotron output to the fundamental waveguide mode ($HE_{11}$ mode) at 170 *GHz*, and the high efficiency coupling was demonstrated for two frequencies. The measured mode purity of $HE_{11}$ mode was 96% at 170 *GHz* and 94% at 137 *GHz* operations with the identical mirrors at the fixed mirror position and angle. The results indicate that the significantly simple dual frequency system can be realized using the gyrotron designed to output the similar beam profiles at multiple frequency operation.

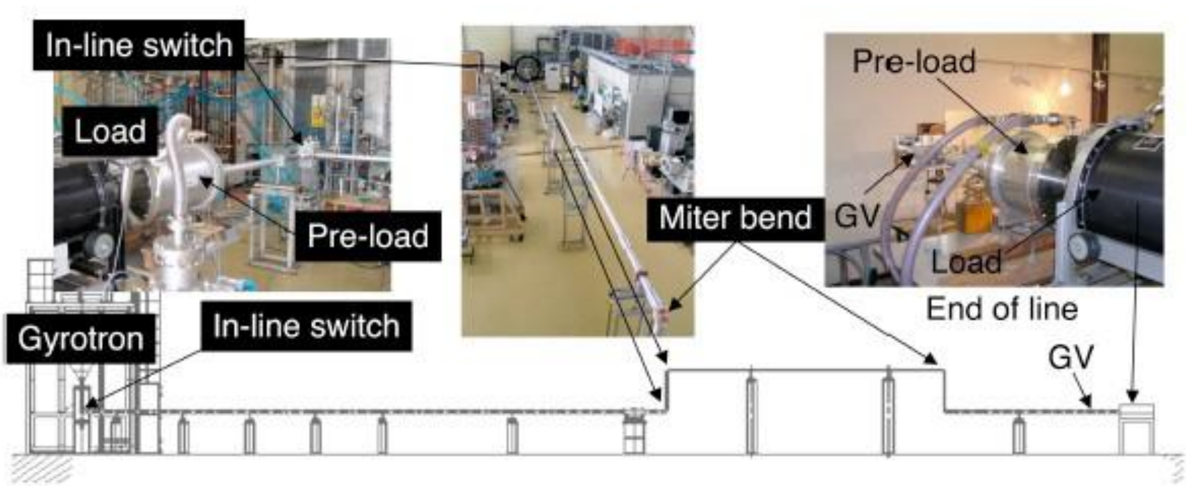


Fig. 10 Pictures and drawings of the transmission line. The waveguide components with the inner diameter of 63.5 *mm* and they are composed of the short and long distance line and they are switched over by an in-line waveguide switch.

### 4-2 Launcher development [36]

The mock-up of the equatorial launcher was fabricated according to the current design to study the mm-wave and mechanical characteristics of the ITER launcher. A cross sectional view of the mm-wave transmission line in the launcher and a picture of the mock-up are shown in Fig.11 and Fig.12, respectively. A blanket shield module made of stainless blocks is equipped for neutron shielding at the top of the launcher. The mm-waves are radiated through the beam duct of the blanket shield. In the experiment, the power was transmitted to the mock-up launcher through the 40 *m* evacuated corrugated waveguide. The mm-wave power is radiated from the corrugated waveguide to the plasma via sequential reflections by fixed mirror and rotational mirror for RF beam steering. The material of the mirrors is Cu. The Gaussian-like beam radiation having a steering capability of 20 degrees-40 degrees from the EL mock-up was also successfully proved. The steering speed of the mirror is 3 s for full angle scan. The power was radiated from one of the 8 waveguides. The radiation power profiles measured at the first and steering mirrors and at the screen placed 2.5 *m* from top of the launcher as shown in Fig.13. Successful power radiation was proved. On the other hand, it was found that some of stray RF propagated in the beam duct and behind the mirrors. It is important to suppress the high order mode in the transmission line to mitigate the heat deposition in the launcher. Prototype tests include the fabrication of mock-ups for the blanket shield modules showed no technological issue on the fabrication and the cooling functionality.

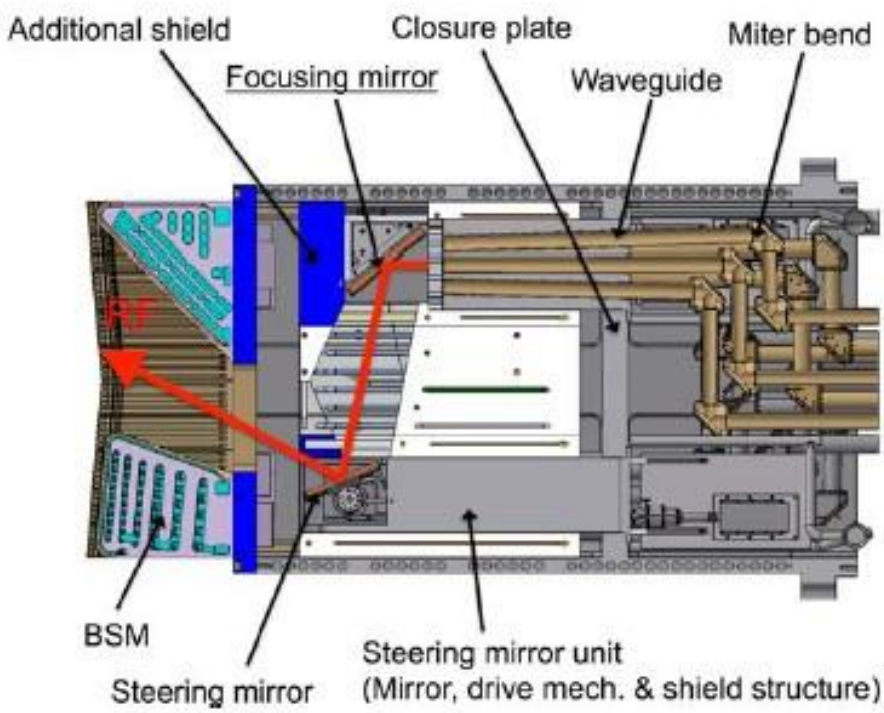


Fig. 11 Cross sectional view of equatorial port launcher.

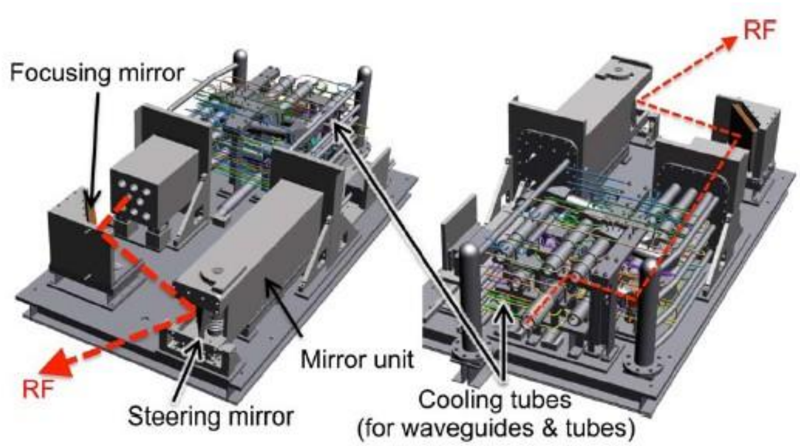


Fig.12 Drawing of the launcher mock-up.

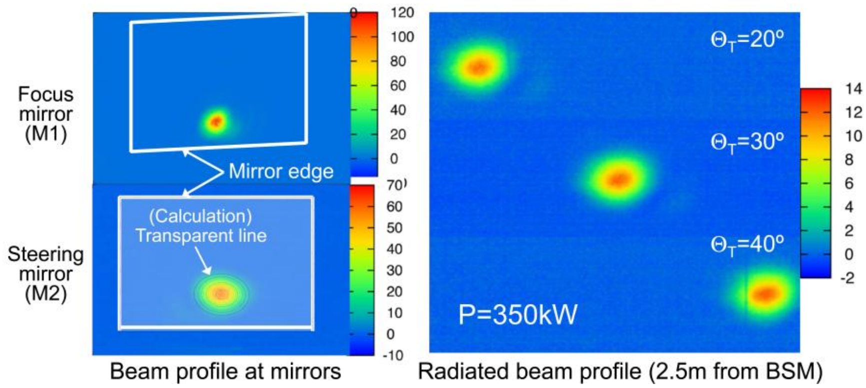


Fig. 13 Radiated pattern of RF beam power at both focus and steering mirror (left) and the location of 2.5 *m* away from the EL mock-up (right)

## 5. Summary

High-power long-pulse gyrotrons are being developed at JAEA. For the application in ITER, after demonstrating the basic requirement of 1 *MW*, >50%, CW-relevant operation, new method was proposed using double anode switches, and 5 *kHz* power modulation was obtained. An advanced mode $TE_{31,11}$ was attempted for even higher power and multi-frequency operation. The 1 *MW* power output was obtained at three frequencies (170 *GHz*/137 *GHz*/104 *GHz*), and high efficiency transmission was demonstrated at these frequencies using the fixed MOU mirrors, which is a demonstration of “ideal” multi-frequency system. Recently, 203 *GHz* Gaussian beam output was also obtained. Fast frequency switching between 170 *GHz* and 167 *GHz* was proved using the super-conducting sweeping coil. For the application in JT-60SA, a final objective of 1 *MW*/100 *s* operation at 138 *GHz*/110 *GHz* was attained. By using the gyrotron as a power source, RF power transmission experiment and launcher development was carried out, and it showed acceptable results for ITER application.

## References

[1] M.Thumm, *J. Infrared Millim Terahertz Waves,* 32, 241 (2011).

[2] G.G.Denisov, et al., *Int. J.Electron.* 72 1079 (1992).

[3] K.Sakamoto, et al., *Phys. Rev. Lett.* 73 3532 (1994).

[4] O.Braz, *Int. J. Infrared Millim. Waves* 18 1495 (1997).

[5] K.Sakamoto, et al., *Rev. Sci. Instrum*., 70, 1 208 (1999).

[6] K.Felch,, et al., J. Phys.:Conf. Ser. 25 13 (2005).

[7] M.Tumm, et al., *IEEE Trans.Electron Devices* 52 818 (2005).

[8] A.V.Chirkov, et al., *Radiophys. Quantum Electron.* 49 344 (2006).

[9] J. Neilson., *IEEE Trans. Plasma Sci.* 34 635 (2006).

[10] M.Thumm, *et al*., *IEEE Trans. Plasma Sci.* 35 1433 (2007).

[11] K.Sakamoto, et al., *NAT Phys.* 3 411 (2007).

[12] K.Sakamoto, et al., *Nucl. Fusion* 49 095019 (2009).

[13] K.Kajiwara, et al., *Fus. Eng. Des.* 86, 955 (2011).

[14] K.Kajiwara, et al., *Applied Physics Express*, 4 126001 (2011).

[15] A.Litvak, et al., *J. Infrared Millim Terahertz Waves,* vol. 32, pp. 337-342 (2011).

[16] K.Kajiwara, et al., *Nucl. Fusion*, 53, 043013 (2013).

[17] H.Zohm, et al., *Nucl. Fusion*, 53, 073019 (2013).

[18] A.Isayama, et al., *Plasma Phys.Control. Fusion*, 42 L37 (2000).

[19] R.Prater, *Phys. Plasmas* 11 2349 (2005).

[20] H.Zohm, *Fus. Sci. and Tech*., 52, 134 (2007).

[21] V.Erckmann *Fus. Eng. Des*., 84 131 (2009).

[22] C.Darbos, *et al. , Fus. Eng. Des.* 84 145 (2009).

[23] T.Omori, et al., *Fus. Eng. Des*. 86, 951 (2011).

[24] K.Takahashi, et al., *Fus.Sci. and Tech.,* 52, 231 (2007).

[25] S.Cirant, *Fus. Sci. and Tech*., 53, 12 (2008).

[26] J.L.Doane, R.A.Olstad, *Fus. Sci. and Tech*., 53, 39 (2008).

[27] J.Lohr, et al., *J. Infrared Millim Terahz Waves* 32 253 (2011).

[28] D.Wagner, et al., *J. Infrared Millim Terahertz Waves,* 32, 274 (2011).

[29] G.G.Denisov, et al., *J. Infrared Millim Terahertz Waves,* 32, 343 (2011).

[30] YS.Bae, private communication.

[31] T.Kobayashi, et al., *to be published in Nuclear Fusion*.

[32] K.Koppenburg, et al, IEEE Trans.on Electron Devices, 48,101 (2001).

[33] R.Hirose, et al., *IEEE Trans. Appl.Supercond.*, 18 920 (2008).

[34] K.Takahashi, et al., *Rev.Sci.Instr.*, 82 063506 (2011).

[35] Y.Oda, et al, *Rev.Sci.Instr.*, 84 013501 (2013).

[36] K.Takahashi, et al, *to be published in Fusion Sci. Tech.*, 67 (2015).